Optical and Quantum Electronics (2018) 50:313
https://doi.org/10.1007/s11082-018-1580-3

Gamma irradiation effects on structural and optical properties of amorphous and crystalline Nb_2O_5 thin films

M. M. El‑Nahass[1] · A. M. Hassanien[2] · Ahmed Ashour[3] · A. Alhuthali[4] · Sultan E. Alomariy[4] · Ateyyah M. Al‑Baradi[4] · A. A. Atta[1,4]

Received: 8 June 2018 / Accepted: 20 July 2018 / Published online: 30 July 2018

Abstract
The structural and optical properties of RF sputtered Nb_2O_5 thin films are studied before and after gamma irradiation. The films are subjected to structural and surface morphological analyses by using X-ray (XRD) and field emission scanning electron microscope techniques. In the wavelength range of 300–2000 nm, the optical parameters for amorphous and crystalline Nb_2O_5 thin films are estimated at differently exposed γ-irradiation doses (0, 50, 100 and 200 kGy). The optical constants, such as optical energy band gap, absorption coefficient, refractive index and oscillators parameters of amorphous and crystalline Nb_2O_5 thin films are calculated. The optical band gaps of γ-irradiated amorphous and crystalline Nb_2O_5 thin films are determined. In the non-absorbing region, the real part of the refractive index of amorphous and crystalline Nb_2O_5 thin films slightly increases with the increase in the exposed γ-irradiation dose.

Keywords Nb_2O_5 thin film · RF sputtering technique · Optical properties · Radiation effect

1 Introduction

Niobium oxides have shown great potential as candidates in a variety of strategic high technology applications such as solid electrolytic capacitors, transparent conductive oxides, photochromic devices, memristors, chemical sensors, counter electrode in electrochromic devices, solar energy applications and display devices (Hunsche et al. 2001; Foroughi-Abari and Cadien 2011; Rani et al. 2014; Mazur et al. 2014; Graça et al. 2015; Nico et al. 2011; Soares et al. 2011; Xiao et al. 2008; Reichmann and Bard 1980; Xia et al. 2007; Gimon-Kinsel and Balkus 1999; Pehlivan et al. 2005; Ozer et al. 1996).

✉ A. A. Atta
aatta08@yahoo.com

1 Department of Physics, Faculty of Education, Ain Shams University, Roxy, Cairo 11757, Egypt

2 Department of Physics, Faculty of Science and Humanity Studies at Al-Quwayiyah, Shaqra University, Al-Quwayiyah 11971, Saudi Arabia

3 National Center for Radiation Research and Technology (NCRRT), Nasr City, Cairo, Egypt

4 Department of Physics, Faculty of Science, Taif University, Taif 888, Saudi Arabia

Niobium-pentoxide (Nb_2O_5) is an n-type semiconductor with a wide band gap of about 3.4 eV. Nb_2O_5 has a thermal stability and mechanical resistance compared to traditional high permittivity materials. It has the most stable oxidation number with the lowest free energy of formation (Hunsche et al. 2001; Foroughi-Abari and Cadien 2011; Rani et al. 2014; Mazur et al. 2014). The structure of Nb_2O_5 has different extensive polymorphism, which gives rise to interesting series of structural phases (Rani et al. 2014). Nb_2O_5 is one of the useful optical materials exhibiting interesting physical properties, such as its stability in air and water, good corrosion resistance in both acid and base media, high refractive index (n = 2.4 at 550 nm), low absorption and high transparency in the UV–Vis–NIR region (Mazur et al. 2014; Graça et al. 2015; Nico et al. 2011).

Gamma radiation is the most energetic, highly penetrating electromagnetic radiation with extremely high frequency. Several studies have been devoted to investigate the influence of gamma irradiation on the physical properties of metal oxide thin films, e.g. In_2O_3, CeO_2, NiO, TeO_2, SiO (Mazur et al. 2014; Graça et al. 2015; Nico et al. 2011; Soares et al. 2011; Xiao et al. 2008; Reichmann and Bard 1980; Xia et al. 2007; Gimon-Kinsel and Balkus 1999; Pehlivan et al. 2005; Ozer et al. 1996; Arshak et al. 2006). The effect of gamma irradiation on structural, optical and electrical properties of thin films of metal oxides and polymers have been extensively studied in the last decade due to the design and development of novel gamma radiation sensors and dosimeters (Lavanya et al. 2017; Yin et al. 2014). The microstructural and morphological properties of metal oxides can be changed due to the exposure to highly energetic ionizing radiations (such as X-ray, beta and alpha particles, gamma irradiation, UV rays, laser, etc.) creating a wide variety of defect states, which in turn can modify their optical, electrical and other physical characterization of solid state materials (Arshak et al. 2006; Lavanya et al. 2017; Yin et al. 2014; Di Sarcina et al. 2014; Gao et al. 2017).

The behavior of Nb_2O_5 thin-film under the irradiation of gamma rays was studied by Di Sarcina et al. (2014). They reported that the optical behavior of Nb_2O_5 thin film was not affected by gamma rays, even at a high dose level (1.79 MGy). The total ionizing dose effects of γ-ray irradiation on Pt/NbO_x/Pt selector devices was investigated using the electrical characterization and XPS technique (Gao et al. 2017). The devices were step irradiated with γ-rays to a maximum dose of 5 Mrad. The experimental results showed that the threshold switching behavior could withstand the 5 Mrad (NbO_2) without any significant changes in the device functionality.

The aim of the present work is to investigate the effects of gamma irradiation of various levels on the structural and optical properties of amorphous and crystalline Nb_2O_5 thin films in order to determine the suitability of these thin films in the gamma radiation dosimetry. To our knowledge, there is no detailed study in the literature about the effect of gamma irradiation on the mentioned behavior of niobium-pentoxide films prepared by the RF sputtering technique.

2 Experimental techniques

Nb_2O_5 thin films were deposited on glass substrates using UNIVEX 350 SPUTTERING UNIT with RF POWER MODEL Turbo drive TD20 classic (Leybold) and thickness monitor model INFICON AQM 160. The ceramic Nb_2O_5 target was purchased from Cathey Advanced Materials Limited. The deposition parameters of Nb_2O_5 thin films are listed in

Table 1. The as-prepared thin films were annealed at 773 K for 6 h in air under normal atmospheric pressure.

The irradiation treatment of the prepared thin films by γ-rays was carried out in ^{60}Co irradiator chamber (Indian cell GC 4000 Å). The irradiation unit consists of annular source permanently enclosed inside a lead shield and cylindrical drawer that can move up and down along the central line. The drawer has a chamber to carry the samples to be irradiated with a dose rate of 10 kGy/100 min.

The field emission scanning electron microscope (FESEM) images were recorded using SEM Model Quanta 250 FEG (Field Emission Gun) attached with EDX Unit (Energy Dispersive X-ray Analyses), with accelerating voltage up to 30 kV, FEI Company, Netherlands. The average film thickness (6576 nm) was determined accurately after deposition by using FESEM as shown in Fig. 1.

X-ray diffraction (XRD) patterns were recorded using Philips X-ray diffractometer model X'Pert with CuK_α (1.5406 Å) radiation operated at 40 kV and 25 mA. The patterns were recorded automatically with a scanning speed of 2 deg/min.

The transmittance, T (λ), and reflectance, R (λ), were measured at normal incidence in the wavelength range 300–2000 nm by means of a double beam spectrophotometer (JASCO model V-670 UV–Vis–NIR) attached with constant angle specular reflection attachment (5°).

The absolute values of T (λ) and R (λ) can be calculated by making a correction to eliminate the absorbance and reflectance of the glass substrate, which is given by the following equations (El-Nahass 1992):

$$T = \left(\frac{I_{ft}}{I_g}\right)(1 - R_g), \quad (1)$$

where I_{ft} and I_g are the intensities of light passing through the film-glass system and that passing through the reference glass, respectively. R_g is the reflectance of the glass substrate and

$$R = \left(\frac{I_{ft}}{I_m}\right)R_m\left(1 + [1 - R_g]^2\right) - T^2 R_g, \quad (2)$$

where I_m is the intensity of light reflected from the reference mirror, I_{fr} is the intensity of light reflected from the sample and R_m is the mirror reflectance.

Table 1 Deposition parameters of Nb_2O_5 thin films used in this study

Material of the target	Nb_2O_5 (99.9% purity)
Substrate	Glass
Substrate temperature (K)	300
Target substrate distance and angle	10 cm with an angle 65°
Target size	3 in. diameter × 5 mm thickness
Deposition rate (nm/min)	4.9
Base pressure (Torr)	2×10^{-6}
Sputtering pressure (mbar)	2×10^{-2}
RF power (W)	150
Pure argon flow rate (sccm; cm^3/min)	20
Average film thickness (nm)	6576

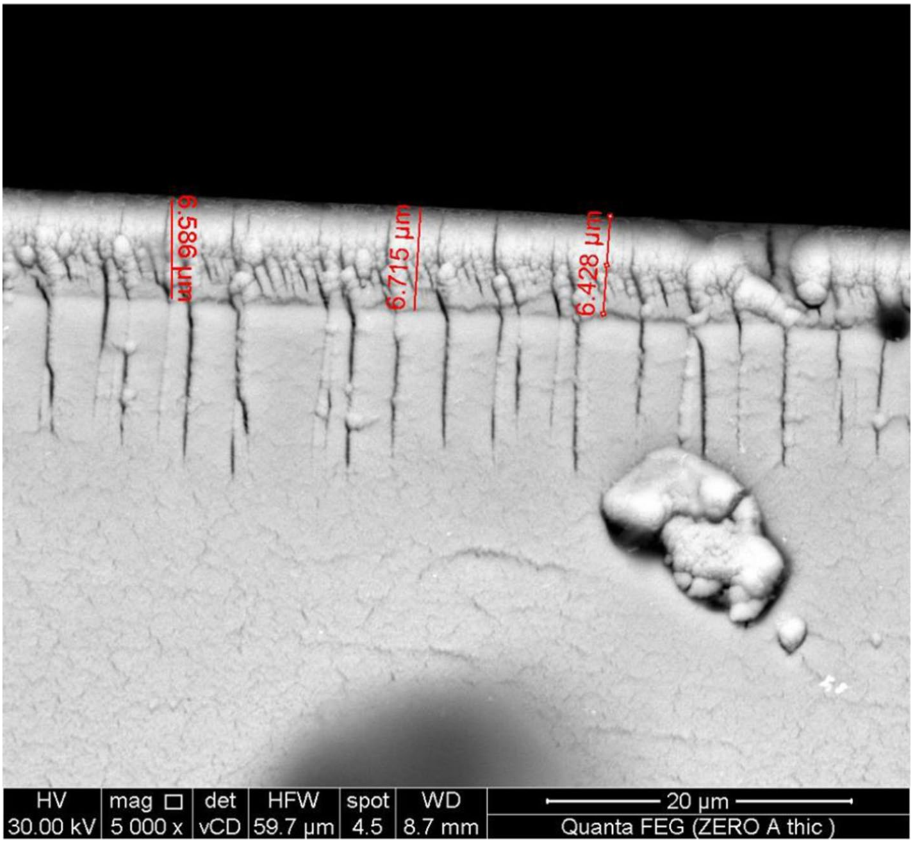

Fig. 1 A FESEM image showing the thickness of the unirradaited amorphous Nb_2O_5 thin film

The optical constants (n and k) were calculated using the same equations described in some previous studies (Di Giulio et al. 1993; El-Nahass et al. 2014). The resultant errors for the n and k parameters were less than ± 4% (see Konstantinov et al. 1998), whereas the errors in the determination of the film thickness and the T (or R) parameter were estimated as ± 2 and ± 1%, respectively.

3 Results and discussion

XRD is used to investigate the effect of gamma irradiation doses on the crystal structure of Nb_2O_5 thin films. Figure 2a represents the XRD patterns of the as-deposited Nb_2O_5 thin films exposed to different γ-irradiation doses. This figure shows that all the films have an amorphous structure. Figure 2b represents the XRD patterns of the annealed Nb_2O_5 thin films (773 K for 6 h) exposed to different γ-irradiation doses. This figure shows that all of the films have a polycrystalline structure; all these peaks were indexed to the JCPDS files no.: 00-028-0317 (Li et al. 2016; Frevel and Rinn 1955; Atta et al. 2017); corresponding to the peseudohexagonal phase (TT-Nb_2O_5). No other phases were identified and the strong peak at $2\theta = 22.57°$ indicates the (001) preferred orientation of the film. It is also observed

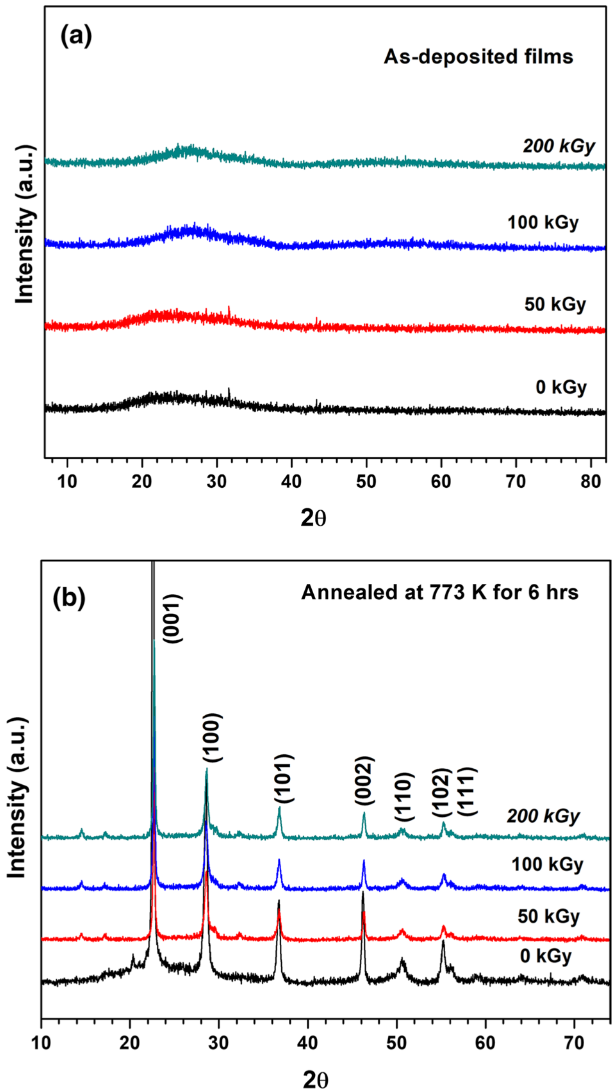

Fig. 2 XRD patterns for amorphous (**a**) and crystalline (**b**) Nb_2O_5 thin films exposed to different γ-irradiation doses

that the peak intensity increases after γ-irradiation confirming the increment in crystallinity after γ-ray exposure. A similar result of partial crystallization has been observed by Arshak et al. (2005) for gamma influenced In_2O_3/SiO structure and Srinivasan et al. (2007) in the case of tin oxide. The significant increase in the crystallinity quality after γ-irradiation could be attributed to the densification occurred due to localized heating developed during the γ-ray exposure (Lavanya et al. 2017).

FESEM micrographs of the amorphous Nb_2O_5 thin film are shown in Fig. 3a–d. These figures show a homogeneous structure of amorphous phase as expected, where the surface morphology is very smooth before and after gamma irradiation. These films exhibit a very poor crystalline structure which was confirmed previously by the XRD analysis.

On the other hand, FESEM micrographs of the crystalline Nb_2O_5 thin film are shown in Fig. 4a–d. These figures clearly show that the surface morphology of all films has a

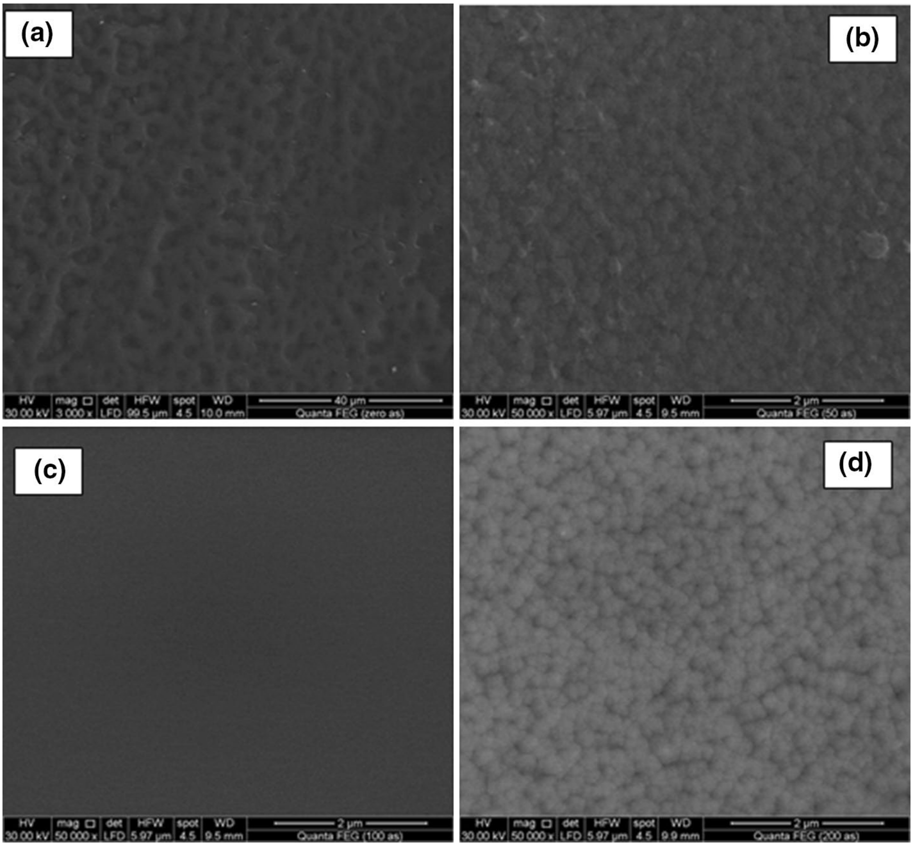

Fig. 3 A FESEM surface images of amorphous Nb_2O_5 thin films exposed to different γ-irradiation doses

homogeneous structure, which indicates a typical crystalline phase. It is also observed that as γ-irradiation dose is increased, the grain size is increased and the agglomeration increases. The average grain size of the crystallites is 30 nm for the non-irradiated film, which is increased to 180 nm for 200 kGy irradiated film.

Figure 5a, b show the optical transmittance T (λ) and reflectance R(λ) for amorphous and crystalline Nb_2O_5 thin films exposed to different γ-irradiation doses. It is observed that the absorption edge for amorphous irradiated Nb_2O_5 thin films shifts towards lower energies region (redshift), while crystalline irradiated Nb_2O_5 thin films shifts towards higher energies region (blue shift).

Figure 6a, b show the spectral distribution of absorption coefficient α (where $\alpha = 4\pi k\ \lambda$) for amorphous and crystalline Nb_2O_5 thin films exposed to different γ-irradiation doses. Figure 6a shows a slight increase in the calculated values of α by increasing the gamma irradiation dose while Fig. 6b shows a slight decrease in the calculated values of α by increasing the gamma irradiation dose.

The energy dependences of the inter-band absorption can be obtained by the following expressions (Abhirami et al. 2013; Alyamani and Mustapha 2016; Alhuthali et al. 2015):

For allowed direct transitions

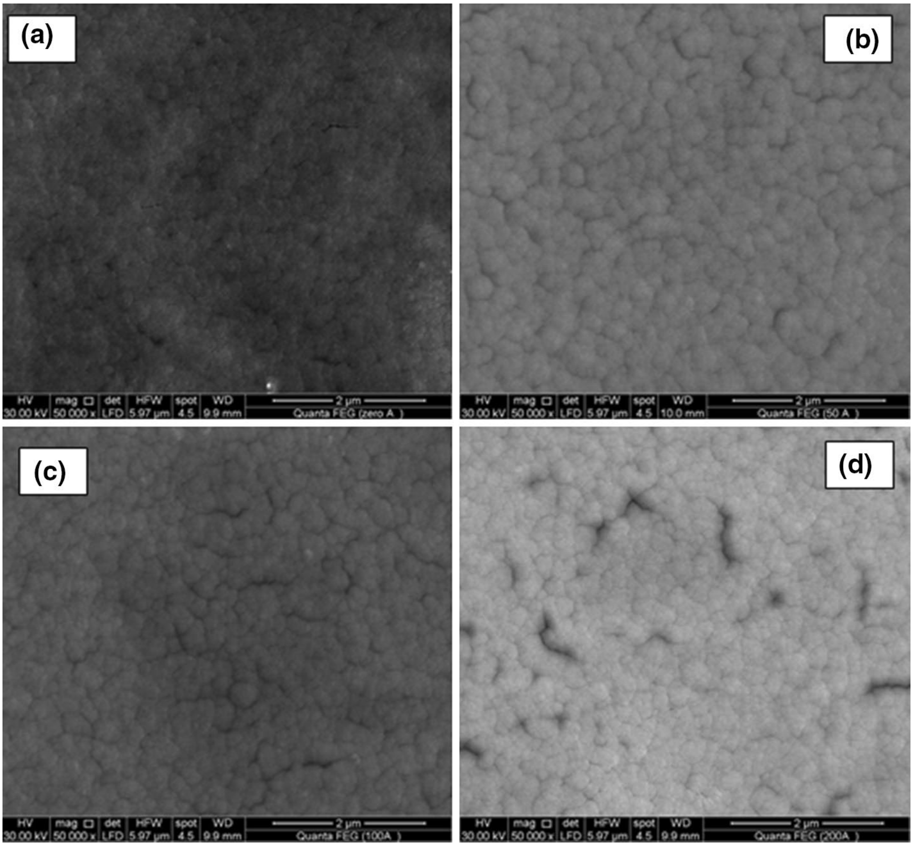

Fig. 4 A FESEM surface images of crystalline Nb_2O_5 thin films exposed to different γ-irradiation doses

$$(\alpha h\upsilon)^2 = A_d\left(h\upsilon - E_g^d\right), \tag{3}$$

For allowed indirect transitions

$$(\alpha h\upsilon)^{1/2} = A_{ind}\left(h\upsilon - E_g^{ind} \mp E_{phonon}\right), \tag{4}$$

where E_g^d and E_g^{ind} represent allowed direct optical energy band gap and allowed indirect optical energy band gap. A_d and A_{ind} are the characteristic parameters, which are, independent of photon energy ($h\upsilon$).

The direct optical energy for both amorphous and crystalline irradiated Nb_2O_5 thin films exposed to different γ-irradiation doses are calculated from the relation between $(\alpha h\upsilon)^2$ versus photon energy (hυ). Figure 7a shows a slight decrease in the optical band gap by increasing gamma irradiation dose in the case of amorphous Nb_2O_5 thin films. The decrease of the optical band gap may be attributed to the formation of localized states due to structural defects (Al-Sofiany and Hassan 2015). Figure 7b shows a slight increase in the optical band gap by increasing gamma irradiation dose in the case of crystalline Nb_2O_5 thin films. This can be related to the improvement of crystallinity which is confirmed by

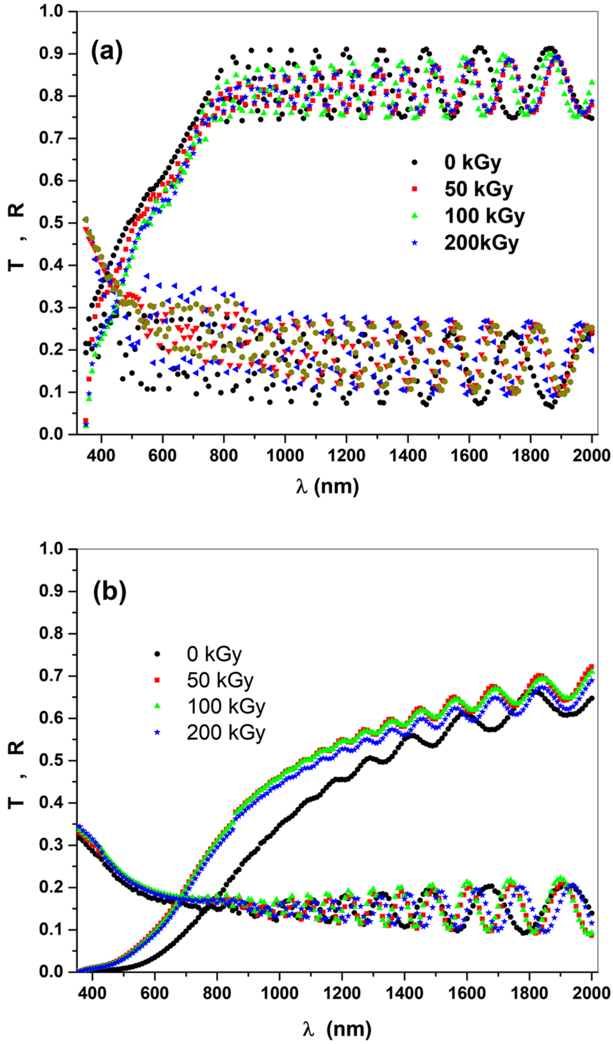

Fig. 5 Optical transmittance T(λ) and reflectance R(λ) of amorphous (**a**) and crystalline (**b**) Nb_2O_5 thin films exposed to different γ-irradiation doses

FESEM and X-ray analyses. The calculated values of allowed direct optical energy band gap for both amorphous and crystalline irradiated Nb_2O_5 thin films are listed in Tables 2 and 3.

It is also expected that, during γ-irradiation, the oxygen vacancies are created within the thin film. At the same time, the oxygen vacancies also get annihilated even under the normal room temperature conditions. This creation and annihilation of oxygen vacancies coexist together and at higher doses of γ-irradiation the number of oxygen vacancies created due to γ-irradiation, may be equal to the number of oxygen vacancies annihilated (Al-Baradi et al. 2014).

The spectral behavior of the refractive indices for amorphous and crystalline Nb_2O_5 thin films exposed to different γ-irradiation doses are shown in Fig. 8a, b respectively. It is found that the values of refractive index slightly increase with the increase of γ-irradiation doses.

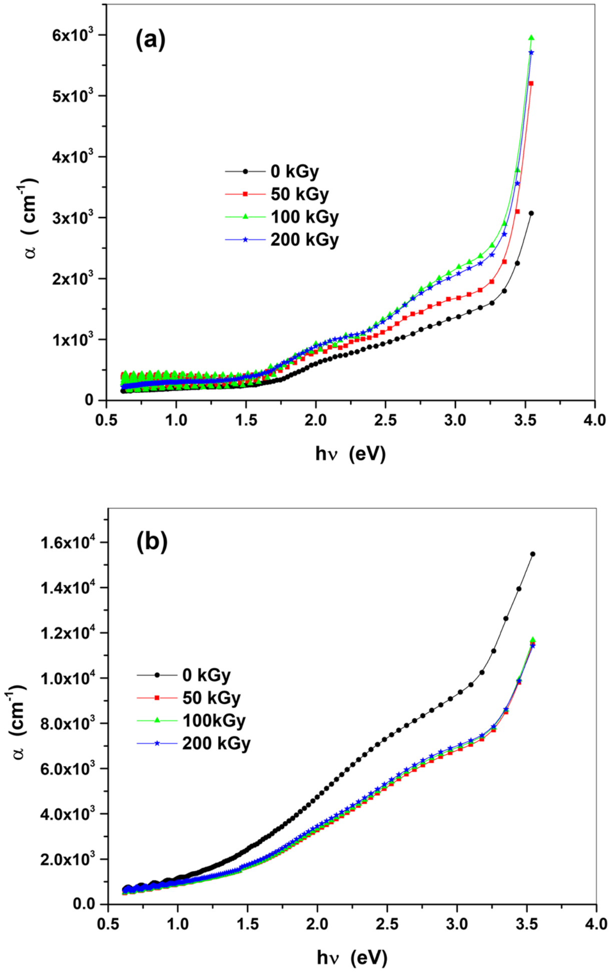

Fig. 6 Variation of (α) as a function of photon energy (hν) for amorphous (**a**) and crystalline (**b**) Nb_2O_5 thin films exposed to different γ-irradiation doses

In the normal dispersion region, the dispersion data of the refractive index has been analyzed using the single effective oscillator model proposed by the Wemple and DiDomenico using the following relation (Wemple and DiDomenico 1971; Wemple 1973).

$$\frac{1}{n^2-1}=\frac{E_0}{E_d}-\frac{1}{E_oE_d}(h\nu)^2, \tag{5}$$

where E_d is the dispersion energy which is a measure of the average strength of interband optical transition and E_o is a single oscillator energy which gives quantitative information on the overall band structure of the material or the "average electronic energy gap" of the transition (Solomon et al. 1988). The dispersion parameters can be estimated by plotting $(n^2-1)^{-1}$ versus $(h\nu)^2$. Figure 9a, b show the relation between $(n^2-1)^{-1}$ versus $(h\upsilon)^2$ for amorphous and crystalline Nb_2O_5 thin films exposed to different γ-irradiation doses. The calculated values of the infinite frequency dielectric constant, ε_∞, E_d and E_o are listed in Tables 2 and 3.

Fig. 7 Variation of $(\alpha h\nu)^2$ as a function of photon energy ($h\nu$) for amorphous (**a**) and crystalline (**b**) Nb_2O_5 thin films exposed to different γ-irradiation doses

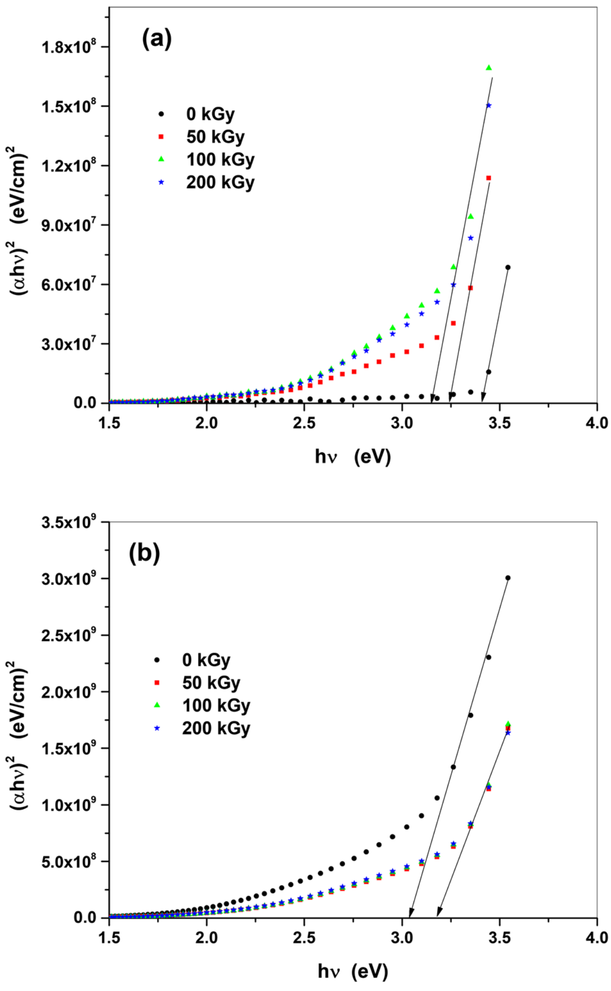

Table 2 Optical parameters of amorphous Nb_2O_5 thin films exposed to different γ-irradiation doses

Optical parameters (kGy)	E_g^d (eV)	E_o (eV)	E_d (eV)	ε_∞	ε_L	N/m^* (10^{46}) (g^{-1} cm^{-3})	N (10^{16}) (cm^{-3})	ω_P (cm^{-1})
0	3.40	4.40	16.44	4.74	5.06	9.66	4.18	2803
50	3.24	4.34	16.90	4.89	5.23	11.40	4.93	3045
100	3.15	4.32	17.37	5.02	5.39	11.80	5.11	3099
200	3.15	4.26	17.67	4.15	5.50	9.87	4.27	2834

In the non-absorbing region, the variation of n^2 versus λ^2 can be obtained by the following relation (Kumar et al. 2000):

$$\varepsilon_1 = n^2 = \varepsilon_L - \frac{e^2 N}{4\pi^2 \varepsilon_o m^* c^2}\lambda^2,$$

Table 3 Optical parameters of crystalline Nb_2O_5 thin films exposed to different γ-irradiation doses

Optical parameters (kGy)	E_g^d (eV)	E_o (eV)	E_d (eV)	ε_∞	ε_L	N/m^* (10^{47}) (g^{-1} cm^{-3})	N (10^{16}) (cm^{-3})	ω_P (cm^{-1})
0 (Atta et al. 2017)	3.03	5.20	21.80	5.21	5.68	1.55	6.73	3556
50	3.16	5.41	23.23	5.29	5.63	1.61	6.98	3621
100	3.16	5.60	24.35	5.35	5.68	1.56	6.77	3567
200	3.16	5.86	25.79	5.41	5.71	1.49	6.46	3484

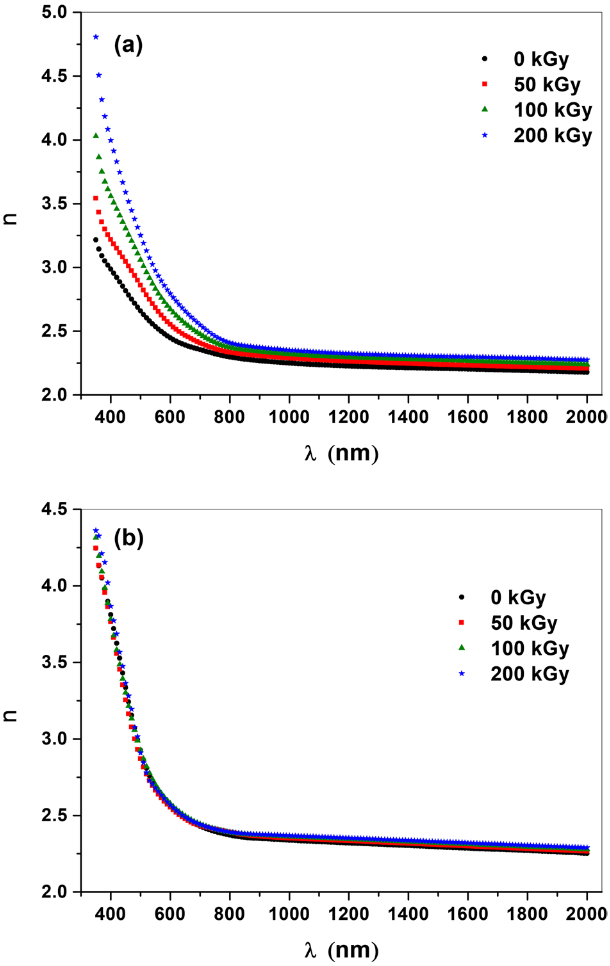

Fig. 8 The refractive index dispersion curves for amorphous (**a**) and crystalline (**b**) Nb_2O_5 thin films exposed to different γ-irradiation doses

where ε_L is the lattice dielectric constant, e is the electronic charge, ε_o is the permittivity of free space, c is the velocity of light and N/m^* is the ratio of free carrier concentration to the effective mass. Figure 10a, b show the relation between n^2 and λ^2 for amorphous and crystalline Nb_2O_5 thin films exposed to different γ-irradiation doses. It is observed that the

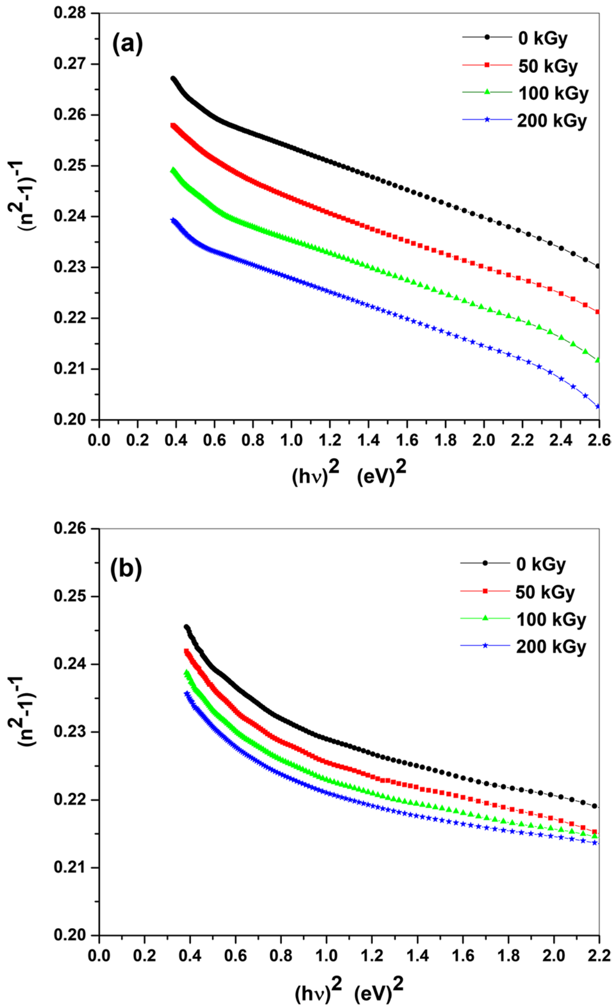

Fig. 9 Relation between $(n^2-1)^{-1}$ and $(h\upsilon)^2$ for amorphous (**a**) and crystalline (**b**) Nb_2O_5 thin films exposed to different γ-irradiation doses

dependence of n^2 on λ^2 is linear at longer wavelengths. Extrapolating this linear part to zero wavelengths gives the value of ε_L and from the slope of this linear part one can get the ratio N/m^*. The obtained dispersion parameters of amorphous and crystalline Nb_2O_5 thin films exposed to different γ-irradiation doses are listed in Tables 2 and 3.

4 Conclusion

The effects of γ-irradiation on the structural and optical properties of amorphous and crystalline RF Sputtered Nb_2O_5 thin films have been investigated. The as-deposited Nb_2O_5 thin films exposed to different γ-irradiation doses have amorphous structure while the annealed Nb_2O_5 thin films (at 773 K for 6 h) exposed to different γ-irradiation doses have a

Fig. 10 Relation between n^2 and λ^2 for amorphous (**a**) and crystalline (**b**) Nb_2O_5 thin films exposed to different γ-irradiation doses

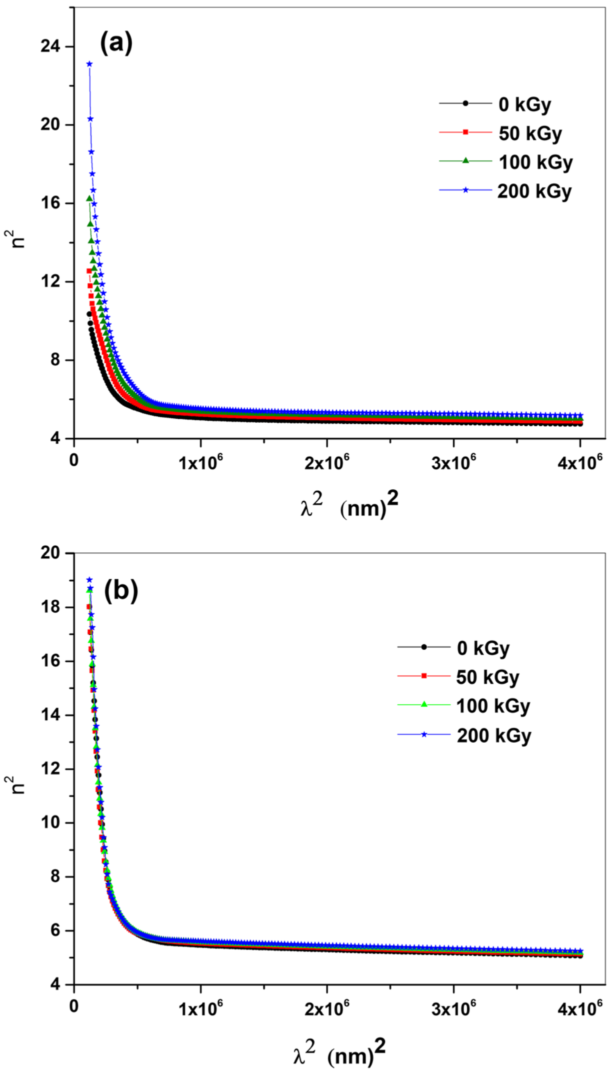

pseudohexagonal phase (TT-Nb_2O_5). FESEM micrographs clearly indicate that the morphological structure of the thin films was highly affected by the γ-radiation exposure. It is found that the average grain size of the crystallites of crystalline Nb_2O_5 thin films increases with the increase of γ-irradiation doses. The optical band gap slightly decreases by increasing gamma irradiation dose for amorphous irradiated Nb_2O_5 thin films while it slightly increases by increasing gamma irradiation dose for crystalline irradiated Nb_2O_5 thin films. The dispersion data of the refractive index has been analyzed using the single effective oscillator model.

References

Abhirami, K.M., Sathyamoorthy, R., Asokan, K.: Structural, optical and electrical properties of gamma irradiated SnO thin films. Radiat. Phys. Chem. **91**, 35–39 (2013)

Al-Baradi, A.M., El-Nahass, M.M., Abd El-Raheem, M.M., Atta, A.A., Hassanien, A.M.: Effect of gamma irradiation on structural and optical properties of Cd_2SnO_4 thin films deposited by DC sputtering technique. Radiat. Phys. Chem. **103**, 227–230 (2014)

Alhuthali, A., El-Nahass, M.M., Atta, A.A., Abd El-Raheem, M.M., Elsabawy, K.M., Hassanien, A.M.: Study of topological morphology and optical properties of SnO_2 thin films deposited by RF sputtering technique. J. Lumin. **158**, 165–171 (2015)

Al-Sofiany, S.M., Hassan, H.E.: Radiation treatment of Cd_2SnO_4 thin films prepared by RF sputtering with different preparation conditions. J. Alloys Compd. **651**, 149–156 (2015)

Alyamani, A., Mustapha, N.: Effects of high dose gamma irradiation on ITO thin film properties. Thin Solid Films **611**, 27–32 (2016)

Arshak, K., Korostynska, O., Henry, J.: Structural modifications in thin films caused by gamma radiation. Mater. Sci. Forum **480–481**, 13–20 (2005)

Arshak, K., Korostynska, O., Molly, J., Harris, J.: Optical radiation sensing properties of MnO/TeO_2 thin films. IEEE Sens. J. **6**, 656–660 (2006)

Atta, A.A., El-Nahass, M.M., Hassanien, A.M., Elsabawy, K.M., Abd El-Raheem, M.M., Alhuthali, A., Alomariy, S.E., Algamdi, M.S.: Effect of thermal annealing on structural, optical and electrical properties of transparent Nb_2O_5 thin films. Mater. Today Commun. **13**, 112–118 (2017)

Di Giulio, M., Micocci, G., Rella, R., Siciliano, P., Tepore, A.: Optical absorption of tellurium suboxide thin films. Phys. Stat. Sol. (a) **136**, K101–K104 (1993)

Di Sarcina, I., Grilli, M.L., Menchini, F., Piegari, A., Scaglione, S., Sytchkova, A., Zola, D.: Behavior of optical thin-film materials and coatings under proton and gamma irradiation. Appl. Opt. **53**, A314–A320 (2014)

El-Nahass, M.M.: Optical properties of tin diselenide films. J. Mater. Sci. **27**, 6597–6604 (1992)

El-Nahass, M.M., Atta, A.A., Abd El-Raheem, M.M., Hassanien, A.M.: Structural and optical properties of DC sputtered Cd_2SnO_4 nanocrystalline films. J. Alloys Compd. **585**, 1–6 (2014)

Foroughi-Abari, A., Cadien, K.C.: Growth, structure and properties of sputtered niobium oxide thin films. Thin Solid Films **519**, 3068–3073 (2011)

Frevel, L.K., Rinn, H.W.: Powder diffraction standards for niobium pentoxide and tantalum pentoxide. Anal. Chem. **27**, 1329–1330 (1955)

Gao, L., Holbert, K.E., Member, S., Yu, S.: Total ionizing dose effects of gamma-ray radiation on NbO_x based selector devices for crossbar array memory. IEEE Trans. Nucl. Sci. **64**, 1535–1539 (2017)

Gimon-Kinsel, M.E., Balkus Jr., K.J.: Pulsed laser deposition of mesoporous niobium oxide thin films and application as chemical sensors. Microporous Mesoporous Mater. **28**, 113–123 (1999)

Graça, M.P.F., Saraiva, M., Freire, F.N.A., Valente, M.A., Costa, L.C.: Electrical analysis of niobium oxide thin films. Thin Solid Films **585**, 95–99 (2015)

Hunsche, B., Vergöhl, M., Neuhäuser, H., Klose, F., Szyszka, B., Matthée, T.: Effect of deposition parameters on optical and mechanical properties of MF- and DC-sputtered Nb_2O_5 films. Thin Solid Films **392**, 184–190 (2001)

Konstantinov, I., Babeva, T., Kitova, S.: Analysis of errors in thin-film optical parameters derived from spectrophotometric measurements at normal light incidence. Appl. Opt. **37**, 4260–4267 (1998)

Kumar, G.A., Thomas, J., George, N., Kumar, B.A., Radhakrishnan, P., Nampoori, V.P.N., Vallabhan, C.P.G.: Optical absorption studies of free (H_2Pc) and rare earth (RePc) phthalocyanine doped borate glasses. Phys. Chem. Glasses **41**, 89–93 (2000)

Lavanya, N., Anithaa, A.C., Sekar, C., Asokan, K., Bonavita, A., Donato, N., Leonardi, S.G., Neri, G.: Effect of gamma irradiation on structural, electrical and gas sensing properties of tungsten oxide nanoparticles. J. Alloys Compd. **693**, 366–372 (2017)

Li, S., Xu, Q., Uchaker, E., Cao, X., Cao, G.: Comparison of amorphous, pseudohexagonal and orthorhombic Nb_2O_5 for high-rate lithium ion insertion. Cryst. Eng. Commun. **18**, 2532–2540 (2016)

Mazur, M., Szymańska, M., Kaczmarek, D., Kalisz, M., Wojcieszak, D., Domaradzki, J., Placido, F.: Determination of optical and mechanical properties of Nb_2O_5 thin films for solar cells application. Appl. Surf. Sci. **301**, 63–69 (2014)

Nico, C., Soares, M.R.N., Rodrigues, J., Matos, M., Monteiro, R., Graça, M.P.F., Valente, M.A., Costa, F.M., Monteiro, T.: Sintered NbO powders for electronic device applications. J. Phys. Chem. C **115**, 4879–4886 (2011)

Ozer, N., Rubin, M.D., Lampert, C.M.: Optical and electrochemical characteristics of niobium oxide films prepared by sol–gel process and magnetron sputtering: a comparison. Sol. Energy Mater. Sol. Cells **40**, 285–296 (1996)

Pehlivan, E., Fatma, Z., Tepehan, G.G.: Effect of TiO_2 mixtures on the optical, structural and electrochromic properties of Nb_2O_5 thin films. Sol. Energy Mater. Sol. Cells **87**, 317–322 (2005)

Rani, R.A., Zoolfakar, A.S., O'Mullane, A.P., Austina, M.W., Kalantar-Zadeh, K.: Thin films and nanostructures of niobium pentoxide: fundamental properties, synthesis methods and applications. J. Mater. Chem. A **2**, 15683–15703 (2014)

Reichmann, B., Bard, A.J.: Electrochromism at niobium pentoxide electrodes in aqueous and acetonitrile solutions. J. Electrochem. Soc. **127**, 241–242 (1980)

Soares, M.R.N., Leite, S., Nico, C., Peres, M., Fernandes, A.J.S., Graca, M.P.F., Matos, M., Monteiro, R., Monteiro, T., Costa, F.M.: Effect of processing method on physical properties of Nb_2O_5. J. Eur. Ceram. Soc. **31**, 501–506 (2011)

Solomon, I., Schmidt, M.P., Sénémaud, C., Khodja, M.D.: Band structure of carbonated amorphous silicon studied by optical, photoelectron, and X-ray spectroscopy. Phys. Rev. B **38**, 13263–13270 (1988)

Srinivasan, S., Patra, M.K., Choudhary, V.S., Pandya, A.: Gamma irradiation study of tin oxide thin films for dosimetric applications. J. Optoelectron. Adv. Mater. **9**, 3725–3728 (2007)

Wemple, S.H.: Refractive-index behavior of amorphous semiconductors and glasses. Phys. Rev. B **7**, 3767–3777 (1973)

Wemple, S.H., DiDomenico Jr., M.: Behavior of the electronic dielectric constant in covalent and ionic materials. Phys. Rev. B **3**, 1338–1350 (1971)

Xia, J.B., Masaki, N., Jiang, K.J., Yanagida, S.: Fabrication and characterization of thin Nb_2O_5 blocking layers for ionic liquid-based dye-sensitized solar cells. J. Photochem. Photobiol. A **188**, 120–127 (2007)

Xiao, X., Dong, G., Xu, C., He, H., Qi, H., Fan, Z., Shao, J.: Structure and optical properties of Nb_2O_5 sculptured thin films by glancing angle deposition. Appl. Surf. Sci. **255**, 2192–2195 (2008)

Yin, K., Liu, S., Cai, Q., Gao, A., Lu, S., Shao, M.: The enhanced ammonia gas-sensing activity of gamma ray irradiated indium vanadate nanoribbons. J. Mater. Sci. Mater. Electron. **25**, 419–422 (2014)